Approximating invertible maps by recovery channels: Optimality and an application to non-Markovian dynamics

Lea Lautenbacher,[1,2,*] Fernando de Melo,[3,†] and Nadja K. Bernardes[1,‡]
[1]*Departamento de Física, Universidade Federal de Pernambuco, PE 50670-901 Recife, Brazil*
[2]*Institut für Theoretische Physik, Albert-Einstein-Allee 11, Universität Ulm, D-89069 Ulm, Germany*
[3]*Centro Brasileiro de Pesquisas Físicas, Rua Doutor Xavier Sigaud 150, 22290-180 Rio de Janeiro, Brazil*

(Received 8 November 2021; accepted 30 March 2022; published 13 April 2022)

We investigate the problem of reversing quantum dynamics, specifically via optimal Petz recovery maps. We focus on typical decoherence channels, such as dephasing, depolarizing, and amplitude damping. We illustrate how well a physically implementable recovery map simulates an inverse evolution. We extend this idea to explore the use of recovery maps as an approximation of inverse maps, and apply it in the context of non-Markovian dynamics. We show how this strategy attenuates non-Markovian effects, such as the backflow of information.

DOI: 10.1103/PhysRevA.105.042421

I. INTRODUCTION

With the advance of quantum computation and quantum communication, the interest in open quantum systems was renewed in the last years. In real-world situations no physical system is completely isolated, and this unavoidable interaction between a system and its environment is responsible for damaging important quantum resources, such as coherence and entanglement. In order to minimize these detrimental effects, one can explore memory effects and backflow of information that may be present in non-Markovian (NM) dynamics [1,2]. Those effects have been extensively controlled and manipulated by recent experimental techniques [3–6].

Another possibility to minimize decoherence effects is to attempt the recovery of the original quantum state or even to revert the noisy process. However, in principle, only unitary dynamics can be perfectly reverted. For noisy situations, different recovery maps have been proposed [7,8]. Especially in the context of quantum error correction, Petz recovery maps [9,10] have been very useful to develop recovery operations [11–19].

The evolution of a quantum system from an initial time zero to a later time t is described by a family of completely positive and trace preserving (CPTP) maps, here denoted by $\Lambda_{t,0}$ with $t \geqslant 0$. As mentioned before, the inverse map, here represented by $\Lambda_{t,0}^{-1}$ in general, is not a valid physical process. There are indeed maps where the inverse is not even mathematically well defined, known as noninvertible maps. Recently it has been shown that the noninvertibility of a map can be explored as a witness of non-Markovianity [20–22]. Note that many interesting physical maps are noninvertible, like a completely depolarizing channel, a completely dephasing channel, and a spontaneous emission.

In this paper, we study optimal recovery strategies exploring the Petz maps. We analyze the behavior of paradigmatic one-qubit quantum channels: dephasing, depolarizing, and amplitude damping. We show how the recovery map can be easily computed and optimized. To measure how well the Petz recovery map recovers a random quantum state, we use the fidelity function as figure of merit. Our numerical analysis elucidates what is the optimum strategy in these cases, even without any initial assumption—as the one required for instance in Ref. [15]. Our analysis allows us to identify that some noninvertible maps can, in principle, be better recovered than others.

As an application, we show how we can explore recovery maps in the context of non-Markovian maps. Markovian evolutions can be defined by a family of maps that are divisible into completely positive (CP) maps, i.e., $\Lambda_{t,0} = \Lambda_{t,s}\Lambda_{s,0}$ for all $t \geqslant s \geqslant 0$. If the inverse of the map is well defined, the intermediate map is given by $\Lambda_{t,s} = \Lambda_{t,0}\Lambda_{s,0}^{-1}$. We explore what would be the consequences of replacing the inverse of the map (a nonphysical map) by a recovery map (a physical map). We show that this evolution still presents backflow of information (a characteristic of non-Markovian evolutions), but in an attenuated way. With this approach we elucidate a subtle characteristic of non-Markovian evolutions: divisibility of the evolution in CP maps is not enough to transform the evolution from non-Markovian to Markovian. The intermediate map $\Lambda_{t,s}$ can only depend on times t and s, and cannot retain any information about previous times.

This paper is structured as follows: we begin by defining in Sec. II reversible, invertible, and recoverable maps. In Sec. III, we optimize the Petz recovery maps for paradigmatic one-qubit decoherence channels. Section IV presents an application of the formalism developed in the previous sections in the context of non-Markovian dynamics. We conclude in Sec. V.

II. REVERSIBLE, INVERTIBLE, AND RECOVERABLE MAPS

The dynamics of quantum systems is generally described by a family of linear completely positive and trace preserving maps. Such CPTP maps model, for instance, noisy dynamics

*lea.lautenbacher@uni-ulm.de
†fmelo@cbpf.br
‡nadja.bernardes@ufpe.br

(open quantum system scenario) and quantum communication channels [23].

Let a quantum system be associated with a Hilbert space $\mathcal{H}$. The set of all possible system states is then $\mathcal{D}(\mathcal{H}) = \{\varrho \in \mathcal{L}(\mathcal{H}) \mid \varrho \geqslant 0,\ \mathrm{tr}(\varrho) = 1\}$, where $\mathcal{L}(\mathcal{H})$ represents the linear operators acting in $\mathcal{H}$. A CPTP map $\Lambda : \mathcal{L}(\mathcal{H}) \mapsto \mathcal{L}(\mathcal{H})$, also called a quantum channel, can be characterized by a set of operators $\{K_i\}$, with each $K_i : \mathcal{H} \mapsto \mathcal{H}$ known as a Kraus operator, as follows:

$$\Lambda(\omega) = \sum_i K_i \omega K_i^\dagger, \tag{1}$$

for all $\omega \in \mathcal{L}(\mathcal{H})$. Such a characterization guarantees the complete positivity of Λ. To be a trace preserving map the Kraus operators must abide by $\sum_i K_i^\dagger K_i = \mathbb{1}$.

When the set of Kraus operators of a given CPTP map is composed by a single element, the trace preservation condition ensures the map to be unitary. In this case the mapping is reversible.. Given a CPTP map $\Lambda : \mathcal{L}(\mathcal{H}) \mapsto \mathcal{L}(\mathcal{H})$, we say it is *reversible* if there exists another CPTP map $\Lambda^* : \mathcal{L}(\mathcal{H}) \mapsto \mathcal{L}(\mathcal{H})$ such that

$$\Lambda^*(\Lambda(\varrho)) = \varrho,\ \forall \varrho \in \mathcal{D}(\mathcal{H}). \tag{2}$$

If Λ is a unitary map, with Kraus operator U acting on $\mathcal{H}$, then Λ^* has Kraus operator $U^\dagger$. In fact, it is easy to show that a CPTP map is reversible if, and only if, it is a unitary map [24].

One way to relax the above definition is to no longer demand the map act on the output of Λ to be CPTP. Given a CPTP map $\Lambda : \mathcal{L}(\mathcal{H}) \mapsto \mathcal{L}(\mathcal{H})$, we say it is *invertible* if there exists another linear map, not necessarily CPTP, $\Lambda^{-1} : \mathcal{L}(\mathcal{H}) \mapsto \mathcal{L}(\mathcal{H})$ such that

$$\Lambda^{-1}(\Lambda(\varrho)) = \varrho,\ \forall \varrho \in \mathcal{D}(\mathcal{H}). \tag{3}$$

Clearly any unitary map is also invertible [25]. However, maps describing noisy dynamics, as the nonfully depolarizing channel (see Sec. III), are invertible but not reversible. This kind of map is most commonly encountered when describing open quantum system dynamics. Note that the fully depolarizing map is not invertible, as it sends all the input states to the maximally mixed state.

Another possible way to relax the definition of reversible maps is by requiring it to hold only for a subset of $\mathcal{D}(\mathcal{H})$. Given a CPTP map $\Lambda : \mathcal{L}(\mathcal{H}) \mapsto \mathcal{L}(\mathcal{H})$, we say it is *recoverable* if there exists another CPTP map $\tilde{\Lambda} : \mathcal{L}(\mathcal{H}) \mapsto \mathcal{L}(\mathcal{H})$ and $\mathcal{S}(\mathcal{H}) \subseteq \mathcal{D}(\mathcal{H})$ such that

$$\tilde{\Lambda}(\Lambda(\varrho)) = \varrho,\ \forall \varrho \in \mathcal{S}(\mathcal{H}). \tag{4}$$

The map $\tilde{\Lambda}$ is dubbed the recovery map of Λ for the subset $\mathcal{S}(\mathcal{H})$ [7]. The unitary map is recoverable, but there are recoverable maps that are not unitary. Other than that, sufficient conditions for the existence of recovery maps for a subset $\mathcal{S}(\mathcal{H})$ is a much studied topic [7–9,11,14–17].

The most well-known class of recovery maps is that of the so-called Petz recovery maps [9]. Given a CPTP map $\Lambda : \mathcal{L}(\mathcal{H}) \mapsto \mathcal{L}(\mathcal{H})$, the corresponding Petz recovery map is a CPTP map defined as

$$\Lambda_P^\sigma(\varrho) := \sigma^{\frac{1}{2}} \Lambda^\dagger(\Lambda(\sigma)^{-\frac{1}{2}}\ \varrho\ \Lambda(\sigma)^{-\frac{1}{2}}) \sigma^{\frac{1}{2}}, \tag{5}$$

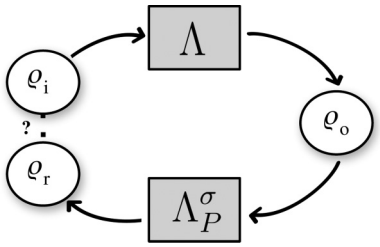

FIG. 1. Schematic representation of a recovery process. An initial state ϱ_i evolves through a noisy channel Λ to a state $\varrho_o = \Lambda(\varrho_i)$. After the evolution a Petz recovery map is applied resulting in $\varrho_r = \Lambda_P^\sigma(\varrho_o)$ with the aim to be as close as possible to ϱ_i.

where $\Lambda^\dagger : \mathcal{L}(\mathcal{H}) \mapsto \mathcal{L}(\mathcal{H})$ is the trace dual of Λ, defined in terms of the Kraus operators $\Lambda^\dagger(\varrho) = \sum_i^n K_i^\dagger \varrho K_i$, and $\sigma \in \mathcal{L}(\mathcal{H})$ is a reference state. If the relative entropy does not change by the action of the map, i.e.,

$$S(\varrho||\eta) = S(\Lambda(\varrho)||\Lambda(\eta))\ \ \forall \varrho, \eta \in \mathcal{S}(\mathcal{H})$$

with $S(\varrho||\eta) = \mathrm{tr}(\varrho \log \varrho - \varrho \log \eta)$, then there exists σ such that $\Lambda_P^\sigma(\Lambda(\varrho)) = \varrho$ for all $\varrho \in \mathcal{S}(\mathcal{H})$.

The actual construction of the recovery channel, i.e., the choice of optimal reference state σ for a given channel Λ and set of states $\mathcal{S}(\mathcal{H})$, is only known for a few "abstract" cases. For instance, it has been shown in Ref. [15] that for an ensemble of commuting density matrices, $\{p_i, \varrho_i\}$, the optimal recovery channel is obtained with the reference state being $\varrho = \sum_i p_i \varrho_i$.

The aim of the present contribution is to investigate the choice of optimal Petz recovery map in physically motivated scenarios. More concretely, given a noisy process described by a non-CP invertible map Λ, what is the best choice of reference state σ that makes Λ_P^σ act as close as possible to a reverse map Λ^*?

This question is schematically explained in Fig. 1. In the forward direction, an input state ϱ_i undergoes the action of a noisy channel Λ, leading to the output state $\varrho_o = \Lambda(\varrho_i)$. In the backward direction, aiming at reversing the effect of the noise, we apply the channel Λ_P^σ recovering the state $\varrho_r = \Lambda_P^\sigma(\varrho_o)$. The question is then how close ϱ_r is from ϱ_i. To quantify this closeness we use the fidelity between the states, $F(\varrho_i, \varrho_r) = ||\sqrt{\varrho_i}\sqrt{\varrho_r}||_1^2$, with the trace norm defined as $||A||_1 = \mathrm{tr}\sqrt{A^\dagger A}$. The optimal reference state, σ^*, is then the one that maximizes the average fidelity over all input states, i.e., $\sigma^* = \mathrm{argmax} F_\Lambda(\sigma)$, where

$$F_\Lambda(\sigma) := \int d\mu_\varrho\ F\big(\varrho, \Lambda_P^\sigma(\Lambda(\varrho))\big), \tag{6}$$

with $d\mu_\varrho$ a uniform measure over the input states.

III. OPTIMAL PETZ RECOVERY MAPS FOR PARADIGMATIC ONE-QUBIT CHANNELS

In this section we numerically obtain the best recovery channel for paradigmatic one-qubit noisy channels, namely, dephasing, depolarizing, and amplitude damping channels. As we do not impose any restriction on the input states, we optimize F_Λ, Eq. (6), over a uniform distribution of mixed input states. In what follows, we generate random one-qubit mixed

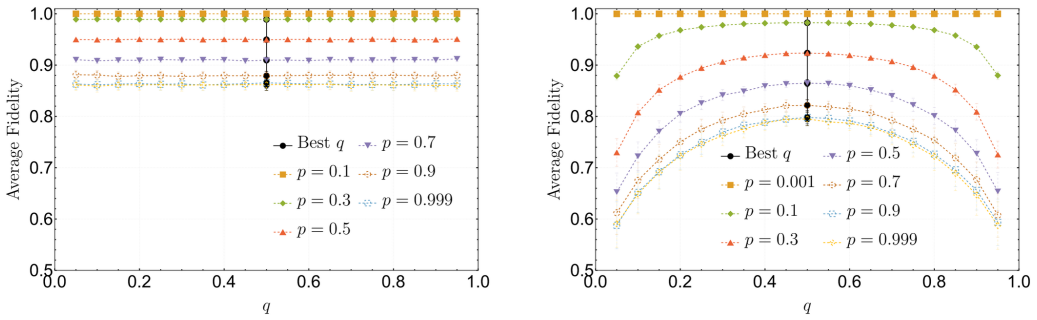

FIG. 2. Average fidelity between an initial state and the recovered state via the Petz map. We took a sample of 10^4 uniformly distributed initial mixed states. The error bars indicate the variance of the fidelity distribution. Different noise parameters p were analyzed for different reference states $[\sigma = (1-q)|0\rangle\langle 0| + q|1\rangle\langle 1|]$ for the dephasing map (left) and the depolarizing map (right). The optimal strategy for each noise strength is marked with a solid black circle.

states, by first generating Haar random two-qubit pure states, followed by the partial trace of the second qubit. Given that we are taking nonunitary processes, and the full state space as input, perfect recovery is impossible. Nevertheless, we can find the best Petz recovery strategy using the optimal mean fidelity as a measure of reversibility for quantum channels.

A. Unital channels: Dephasing and depolarizing

Unital quantum channels are those that map the maximally mixed state onto itself, $\Lambda(\mathbb{1}/2) = \mathbb{1}/2$. In other words, the maximally mixed state is a fixed point for these maps. Two of the most important unital channels are the dephasing and the depolarizing noisy channels.

The dephasing channel, Λ_{deph}, destroys the relative phase information between the computational basis states, being one the most prevalent types of noises in physical realizations. The depolarizing channel, Λ_{depo}, can be seen as noise that probabilistically changes the system state by the maximally mixed state. Mathematically, these channels are modeled as follows:

$$\Lambda_{\text{deph}}(\varrho) = \left(1 - \frac{p}{2}\right)\varrho + \frac{p}{2} Z\varrho Z, \tag{7}$$

$$\Lambda_{\text{depo}}(\varrho) = \left(1 - \frac{3p}{4}\right)\varrho + \frac{p}{4}(X\varrho X + Y\varrho Y + Z\varrho Z). \tag{8}$$

In the equations above, $p \in [0, 1]$ is a parameter that characterizes the noise strength ($p = 0$, no noise; $p = 1$, maximal noise), and X, Y, and Z are the usual Pauli matrices.

We want to determine the optimal recovery channel for such noise models, fixing a noise strength p and taking as input a uniform distribution over all mixed states. Given that we are taking a uniform measure over mixed states, and that the channels are unital, it is expected that the best Petz recovery map is obtained by taking the reference state as the maximally mixed one. This is numerically confirmed by parametrizing the reference state as

$$\sigma = (1-q)|0\rangle\langle 0| + q|1\rangle\langle 1|, \tag{9}$$

with $q \in [0, 1]$, and evaluating the average fidelity as a function of q for both channels. The above parametrization is immediately suggested by the azimuthal symmetry of the output distribution of states for both noisy channels. As it is clear from Fig. 2, taking $q = 1/2$, i.e., choosing the reference state as the maximally mixed one, is always an optimal choice for the dephasing and depolarizing channels. For the dephasing channel, as all the states of the form of σ are preserved, any value of q is also an optimal choice (see Appendix A for the explicit calculation).

Using the maximally mixed state as reference state, and the unitality of such maps, we obtain that

$$\Lambda_P^{\mathbb{1}/2}(\varrho) = \Lambda^\dagger(\varrho).$$

Noticing furthermore that the dephasing and depolarizing noise models are self-dual ($\Lambda^\dagger = \Lambda$), we reach the conclusion that the optimal Petz recovery map for these noise models is again the noisy map. As such, no recovery is actually obtained. In fact, it is clear from this discussion that to take the identity channel as a "recovery map" is more advantageous than taking the optimal Petz map when considering the set of all single qubit states as input. This conclusion is illustrated in Fig. 3, where we compare the optimal Petz map, for a given p, with two other strategies: first, the strategy of using an identity map as recovery map, i.e., to simply "return" the output state $\Lambda_{\text{deph/depo}}(\varrho)$ as the best approximation for ϱ; second, we take as a recovery map the fully depolarizing map, i.e., independently of the output state $\Lambda_{\text{deph/depo}}(\varrho)$ we return the maximally mixed state. From Fig. 3, the latter is clearly the worst strategy, despite the fact that the maximally mixed state is indeed the average state for the input distribution of states [15].

B. Nonunital channel: Amplitude damping

For nonunital channels, the choice of the optimal reference state for the Petz recovery map is not so obvious. As an example of a nonunital channel we analyze the amplitude damping channel. Such a channel models the spontaneous decay of a two-level atom when interacting with a zero-temperature environment. Mathematically, the amplitude damping channel can be written in the Kraus form as

$$\Lambda_{\text{AD}}(\varrho) = K_0(p)\varrho K_0^\dagger(p) + K_1(p)\varrho K_1^\dagger(p),$$

with Kraus operators

$$K_0(p) = \begin{pmatrix} 1 & 0 \\ 0 & \sqrt{1-p} \end{pmatrix}, \quad K_1(p) = \begin{pmatrix} 0 & \sqrt{p} \\ 0 & 0 \end{pmatrix}. \tag{10}$$

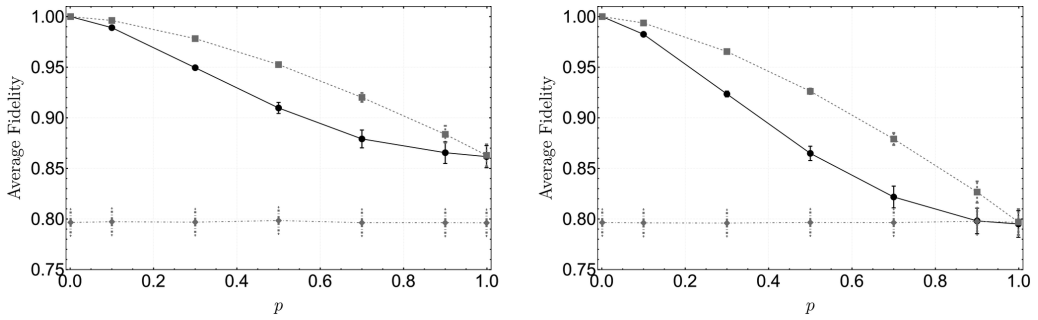

FIG. 3. Average fidelity—dephasing (left) and depolarizing (right)—between the initial state and the state recovered by different strategies: the identity channel (dotted line), optimal Petz map (solid line), and always returning the maximally mixed state (dot-dashed line). Plot in terms of the noise parameter p. We took a sample of 10^4 uniformly distributed mixed states. The variance of the fidelity distribution is indicated by the error bars.

Again the parameter $p \in [0, 1]$ quantifies the noise strength. Taking $p = 0$ there is no decay, while for $p = 1$ the system is left in the "ground state" $|0\rangle\langle 0|$.

Despite the fact that the amplitude damping channel is not unital, it maps a uniform distribution of states onto a distribution which is invariant under rotations around the z axis of the Bloch sphere. Given that, it is reasonable to suppose that the optimal Petz recovery channel is obtained with a reference state that is located on the z axis, i.e., the optimal reference state can be written as in the state in Eq. (9). In Fig. 4 we use this parametrization to numerically obtain the best reference state for different values of the noise strength p.

From Fig. 4 we see that for weak amplitude damping the best reference state is the $|0\rangle\langle 0|$ state. As the noise strength increases, the best reference state moves towards the maximally mixed state. To understand that, we compare the optimal Petz map, for a given p, with the previous strategies: the identity map as the recovery map [always returning $\varrho_r = \Lambda_{\mathrm{AD}}(\varrho)$], and returning $\varrho_r = \mathbb{1}/2$ independently of the initial state. The comparison among these strategies is shown in Fig. 5.

As it can be seen from Fig. 5, for very weak amplitude damping the best Petz recovery map (with reference state around $|0\rangle\langle 0|$) is equivalent to the identity map. This is expected, as the state $\Lambda_{\mathrm{AD}}(\varrho)$ should be very close to ϱ for small p's. For strong amplitude damping the state $\Lambda_{\mathrm{AD}}(\varrho)$ loses almost all the information about ϱ. In this case the optimal Petz recovery map (with reference state around $\mathbb{1}/2$) is equivalent to a fully depolarizing map—when no information is available, the unbiased choice is to return the maximally mixed state. It is however interesting to notice that for intermediate noise strengths the optimal Petz recovery map is better than the other strategies.

Note that, fixing a strategy, by comparing Figs. 3 and 5, the average fidelity for the dephasing map is always higher. Thus, in this context, we can conclude that the dephasing channel can be better recovered. This is related to the image set of each evolution. Because of the symmetry of the dephasing process, it can be said that some information is still available after the decoherence process.

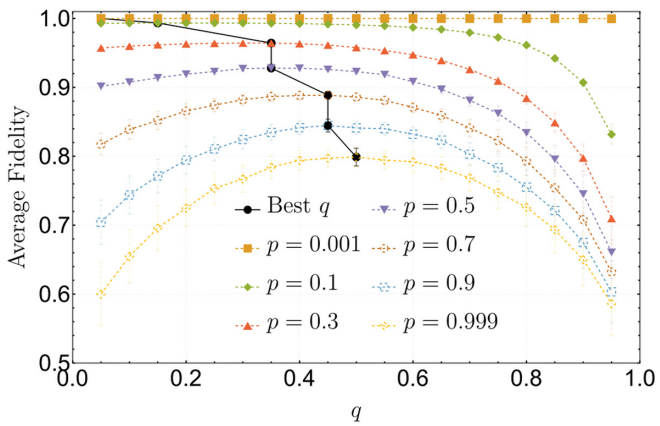

FIG. 4. Average fidelity between the initial state and the recovered state via the Petz map for the amplitude damping map. We took a sample of 10^4 uniformly distributed mixed states. The variance of the fidelity distribution is indicated by the error bars. Different noise parameters p were analyzed for different reference states ($\sigma = (1 - q)|0\rangle\langle 0| + q|1\rangle\langle 1|$). The optimal strategy for each noise strength is marked with a solid black circle.

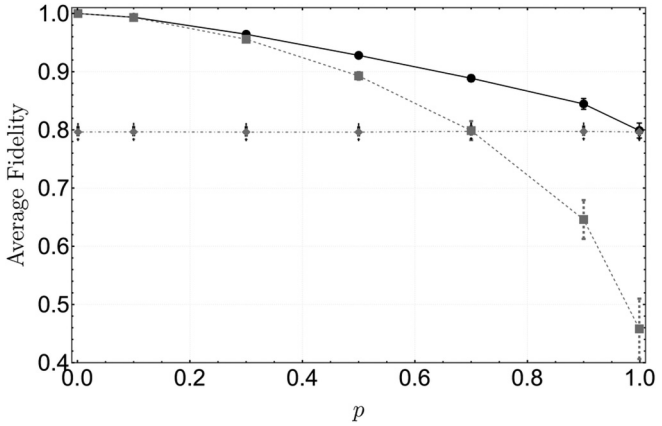

FIG. 5. Average fidelity for the amplitude damping map between the initial and the state recovered by different strategies: the identity channel (dotted line), optimal Petz map (solid line), and always returning the maximally mixed state (dot-dashed line). Plot in terms of the noise parameter p. We took a sample of 10^4 uniformly distributed mixed states. The variance of the fidelity distribution is indicated by the error bars.

IV. RECOVERY CHANNELS APPLIED TO NON-MARKOVIAN DYNAMICS

With the results of the previous section in hand, now we exploit the impact of recovery channels in non-Markovian dynamics.

Formally, we will consider the definition of Markovianity as the divisibility of the maps. A family of dynamical maps $\Lambda_{t,0}$ is divisible if it can be expressed as a composition of linear maps:

$$\Lambda_{t,0} = \Lambda_{t,s}\Lambda_{s,0} \quad \text{for all } t \geqslant s \geqslant 0. \tag{11}$$

The dynamics is called Markovian, or CP divisible, if the intermediate map $\Lambda_{t,s}$ is CPTP for all $t \geqslant s \geqslant 0$ [1]. Note that if $\Lambda_{s,0}$ is invertible then one can obtain $\Lambda_{t,s}$ as

$$\Lambda_{t,s} = \Lambda_{t,0}\Lambda_{s,0}^{-1}. \tag{12}$$

Two points should, however, be noticed. First, as the inverse of a map is in general not completely positive, then the complete positivity of $\Lambda_{t,s}$ is not guaranteed. Second, for Eq. (12) to be consistent, $\Lambda_{s,0}^{-1}\Lambda_{s,0} = \mathbb{1}$, as defined in Eq. (3).

Usually non-Markovian dynamics are associated with a backflow of information [1,26]. One of the common witnesses of this backflow of information is the distinguishability between two states. Thus, a subset of states will become relevant and the use of a Petz recovery map is then justified in this scenario.

Here we will then employ Petz recovery maps to obtain approximations for $\Lambda_{t,s}$, i.e., in Eq. (12) we change $\Lambda_{s,0}^{-1}$ by $\Lambda_{P0,s}^{\sigma}$:

$$\Phi_{t,s,0} = \Lambda_{t,0}\Lambda_{P0,s}^{\sigma}. \tag{13}$$

Clearly this map is CP, as it is formed by a composition of CP maps. As such, if now we designate the total approximated map by

$$\Lambda_{t,0}^{\text{approx}} = \Phi_{t,s,0}\Lambda_{s,0}, \tag{14}$$

then it will be also, by construction, a CP map. However, as $\Phi_{t,s,0}$ may depend on the time interval $[0, s]$, the map $\Lambda_{t,0}^{\text{approx}}$ is not necessarily CP divisible, i.e., it is not necessarily Markovian. Note that $\Lambda_{t,0}^{\text{approx}} = \Lambda_{t,s}\Lambda_{s,0}\Lambda_{P0,s}^{\sigma}\Lambda_{s,0}$, so the non-CP map $\Lambda_{t,s}$ is still contained in $\Lambda_{t,0}^{\text{approx}}$ and this is the reason why the approximated map is not CP divisible. Below, we analyze how well $\Lambda_{t,0}^{\text{approx}}$ approximates $\Lambda_{t,0}$, and compare the non-Markovianity of both channels.

Non-Markovian dephasing models

To analyze the impact of using the Petz recovery map to obtain an approximated channel, we will exploit two dephasing, Eq. (7), non-Markovian models. The reference state, from here on, will thus be set to the maximally mixed one.

For the first model, named here "case 1," we construct a non-Markovian evolution by setting a time-dependent error probability as

$$p_1(t) = \alpha(1 - e^{-2(1-\cos\omega t)}), \tag{15}$$

where $\alpha = e^4/(e^4 - 1)$, and ω is a system natural frequency (see Fig. 6). This is a periodic function with period 2π, fully characterized in terms of the Lindblad local generator with negative rates [27] (an explicit derivation is given in Appendix B). A state ϱ undergoing this evolution reaches the maximally dephased state when $\omega t = (2n + 1)\pi$, with $n \in \mathbb{N}$.

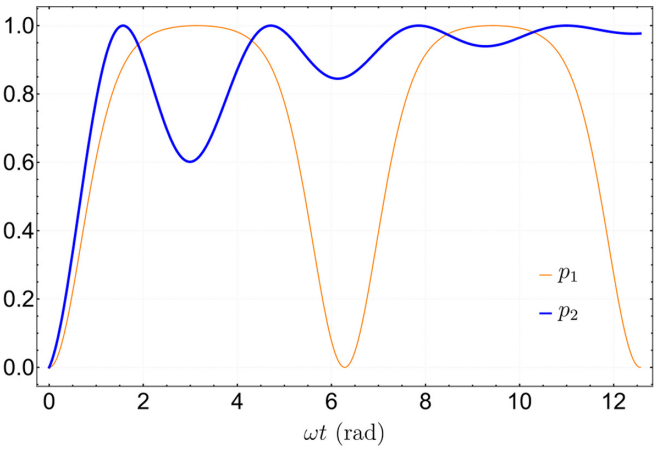

FIG. 6. Probabilities p_1 (case 1, orange line) and p_2 (case 2, blue thick line) vs ωt.

For the second model, named "case 2," the error probability will be defined as

$$p_2(t) = 1 - e^{-0.3\omega t}\cos^2\omega t. \tag{16}$$

In this case, a system undergoing this evolution reaches the maximally dephased state, goes back to an intermediate state between the maximally dephased and the initial one, and repeats the process, with the intermediate state even being closer to the maximally dephased than before. When ωt goes to infinity, the system reaches its maximally dephased state. Both probabilities p_1 and p_2 are displayed in Fig. 6.

We start our analysis by observing the so-called information backflow that can appear in NM dynamics [1,26]. Concretely, take the trace distance $D(\varrho_1, \varrho_2) = 1/2||\varrho_1 - \varrho_2||_1$ between two states as a quantifier of their distinguishability. For a NM dynamics it can be that $D(\Lambda_{t,0}(\varrho_1), \Lambda_{t,0}(\varrho_2)) \leqslant D(\Lambda_{t',0}(\varrho_1), \Lambda_{t',0}(\varrho_2))$, for $t' \geqslant t$. This should be contrasted with the Markovian case, where $D(\Lambda_{t,0}(\varrho_1), \Lambda_{t,0}(\varrho_2)) \geqslant D(\Lambda_{t',0}(\varrho_1), \Lambda_{t',0}(\varrho_2))$ for all $t' \geqslant t$.

In Fig. 7 we compare, for both dephasing models, the information backflow of the original map with the corresponding approximated versions. In all the cases, as initial states we took $\varrho_1 = |+\rangle\langle+|$ and $\varrho_2 = |-\rangle\langle-|$, as these states are orthogonal and consequently optimal states to detect information backflow. For simplicity, we have fixed the final time as twice the intermediate time in Eq. (14), i.e., $s \mapsto t$ and $t \mapsto 2t$. From Fig. 7, it is clear that the approximated dynamics are also non-Markovian, as both present information backflow. It is also evident that the non-Markovianity strength in both approximated cases is decreased when compared with the original maps. In case 1 the recovery of distinguishability is almost completely destroyed. On the other hand, in case 2, the complete backflow is still present in the approximated case. It is only a matter of waiting a longer time, but a similar backflow is present in the approximate and original dynamics.

In order to have a state-independent characterization, now we directly compare the original, $\Lambda_{2t,0}$, and approximated channels, $\Lambda_{2t,0}^{\text{approx}}$, for both models.

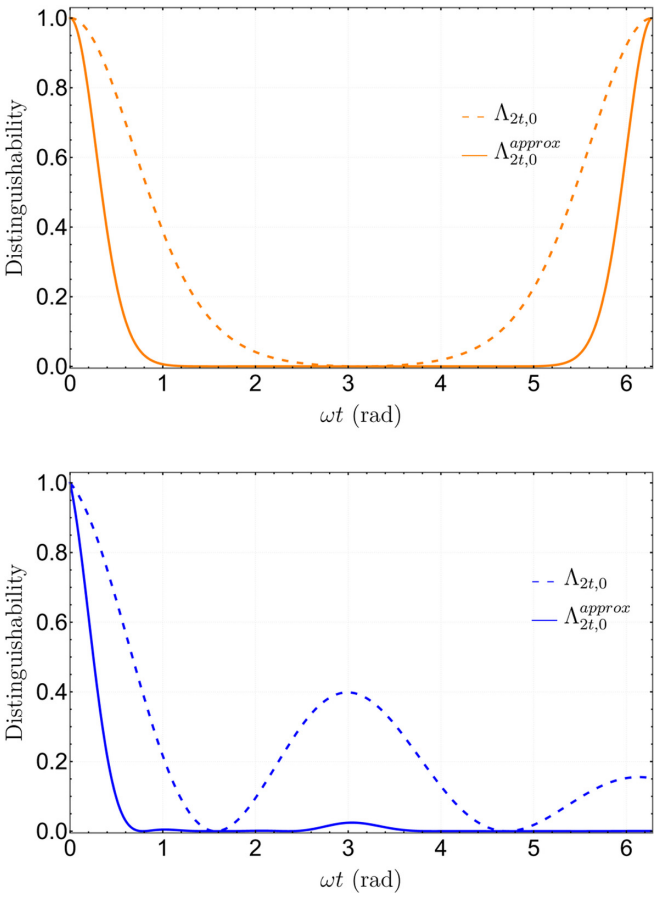

FIG. 7. Distinguishability between two states $D(\varrho_1(t), \varrho_2(t))$ vs time, with initial states $\varrho_1 = |+\rangle\langle+|$ and $\varrho_2 = |-\rangle\langle-|$, for case 1 (top) and case 2 (bottom), where $\varrho_i(t) = \Lambda_{2t,0}(\varrho_i)$ (dashed line) and $\varrho_i(t) = \Lambda_{2t,0}^{\text{approx}}(\varrho_i)$ (solid line) with $i = 1, 2$.

To quantify the distance between the maps we evaluated the trace distance between their Choi matrices:

$$\left\| J\left(\Lambda_{2t,0}^{\text{approx}}\right) - J(\Lambda_{2t,0}) \right\|_1, \tag{17}$$

where $J(\Lambda) = (\mathbb{1} \otimes \Lambda)(|\Omega\rangle\langle\Omega|)$ is the Choi matrix of Λ with $|\Omega\rangle = \frac{1}{\sqrt{2}} \sum_{i=0}^{1} |i\rangle \otimes |i\rangle$ a maximally entangled state. The norm of the Choi matrix, also known as the dynamical matrix, is widely used to quantify the degree of noncomplete positiveness of a map [28,29]. The results are shown in Fig. 8.

Combining the results shown in Figs. 7 and 8, one interesting observation emerges. For a fixed value for the distances between the original and approximated maps, the recovery of the information backflow can be very different. For example, in Fig. 8, the distances between the dynamics at $\omega t = 5.9$ rad (case 1) and $\omega t = 3.1$ rad (case 2) are almost the same; however, the information backflow displayed by the approximated channel in case 1 is closer to the original backflow than what is recovered in case 2, as can be seen in Fig. 7. In experimental implementations such a result implies that approximations within a fixed distance from the theoretical dynamics may lead to very different behavior of non-Markovian features. In other words, the information backflow is not a robust non-Markovian feature.

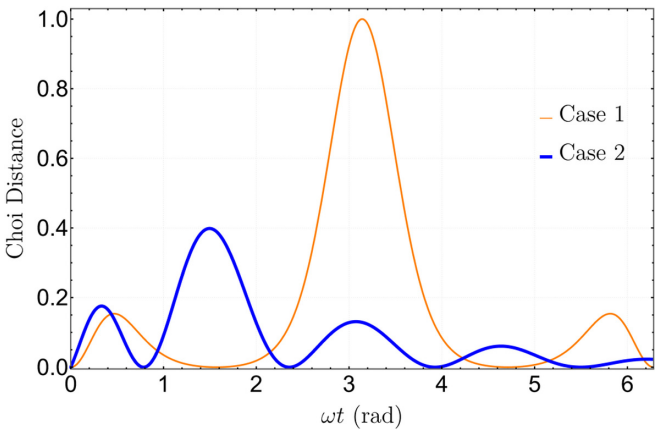

FIG. 8. Normalized Choi distance $||J(\Lambda_{2t,0}^{\text{approx}}) - J(\Lambda_{2t,0})||_1$ between the original $\Lambda_{2t,0}$ and approximated channels $\Lambda_{2t,0}^{\text{approx}}$ vs time for case 1 (orange line) and case 2 (blue thick line).

V. CONCLUSION

In this paper we have explored the use of the Petz recovery map in a general context. We established the best Petz map for paradigmatic one-qubit channels (unital and nonunital) optimizing the reference states. When using as input the full set of single qubit states, we showed that the optimal Petz recovery map is worse than simply returning the output state, i.e., to use the identity channel as "recovery channel." We also showed that among the strategies analyzed the dephasing channel is the decoherence channel that can be better recovered in terms of the average fidelity between the initial and the recovered state.

The Petz recovery map has been also explored in the context of non-Markovian evolution. We approximated the inverse of the map $\Lambda_{s,0}$ by its optimal Petz recovery map, and showed that the approximated evolution still presents backflow of information, but in an attenuated way. We also analyzed how the distance between the actual dynamics and the approximated one impacts on the backflow of information. We observed that equally good approximations might lead to drastically different behaviors for the backflow of information. This can be especially interesting for experimental implementations of non-Markovian evolutions, and for the use of non-Markovianity in the context of hiding and retrieving information, as in a quantum vault [30].

ACKNOWLEDGMENTS

We gladly acknowledge fruitful discussions with Gabriel Landi, and thank Mark M. Wilde and Carlos Pineda for a careful reading of an earlier version of this paper. This work is supported by the Brazilian funding agencies CNPq and CAPES, and it is part of the Brazilian National Institute for Quantum Information.

APPENDIX A: OPTIMAL PETZ RECOVERY MAP: DEPHASING CHANNEL

In this Appendix we analytically show that the optimal Petz recovery map for the dephasing noise is obtained with an arbitrary value of the parameter q in the reference state (9).

The first thing to notice is that σ is diagonal in the computational basis. As such, it does not suffer the influence of the dephasing channel:

$$\Lambda_{\text{deph}}(\sigma) = \sigma, \quad \forall 0 \leqslant q \leqslant 1. \tag{A1}$$

Also due to this diagonal property, it is simple to obtain the reference state's square roots:

$$\sigma^{\pm\frac{1}{2}} = (1-p)^{\pm\frac{1}{2}}|0\rangle\langle 0| + p^{\pm\frac{1}{2}}|1\rangle\langle 1|. \tag{A2}$$

Now, let $\varrho = [\varrho_{ij}]$, with $i, j \in \{0, 1\}$, be a generic single qubit state. Using the results above, and remembering that the dual channel of the dephasing map is the dephasing map itself, it is now simple to show that the Petz recovery map (5) for the present case is such that

$$\Lambda_P^{\sigma}(\varrho) = \Lambda_{\text{deph}}(\varrho). \tag{A3}$$

From the equation above, we then conclude that the Petz recovery map for the dephasing channel, with reference state σ as in (9), is independent of the parameter q. In this way, any choice of q will lead to the same recovered state.

APPENDIX B: TIME-LOCAL GENERATOR

A random unitary dynamical map

$$\Lambda_t(\varrho) = \sum_{k=0}^{3} p_k(t)\sigma_k\varrho\sigma_k \tag{B1}$$

can be fully characterized in terms of a local generator given by

$$\mathcal{L}(\varrho) = \sum_{k=1}^{3} \gamma_k(t)(\sigma_k\varrho\sigma_k - \varrho), \tag{B2}$$

where $\gamma(t)$ are the decoherence rates and σ_1, σ_2, and σ_3 are the Pauli matrices. Using the framework developed in Ref. [27], a random unitary dynamics is Markovian if and only if

$$\gamma_1(t) \geqslant 0, \quad \gamma_2(t) \geqslant 0, \quad \gamma_3(t) \geqslant 0, \quad \text{for all } t \geqslant 0. \tag{B3}$$

In order to obtain a non-Markovian evolution, we choose decay rates that can assume negative values, $\gamma(t_i) < 0$ for some t_i. If the dynamics has only one decoherence channel, i.e., only one decoherence rate is nonvanishing, γ_k, the time dependent probabilities can be obtained by

$$p_k(t) = \tfrac{1}{2}[1 - e^{-2\Gamma_k(t)}], \tag{B4}$$

where $p_0(t) = 1 - p_k(t)$ and

$$\Gamma_k(t) = \int_0^t \gamma_k(\tau)d\tau. \tag{B5}$$

For the first dephasing model defined in Sec. IV, we chose $\gamma(t) = \sin(t)$. From the equations above we easily obtain

$$p_t = \alpha(1 - e^{-2[1-\cos(t)]}), \tag{B6}$$

where $\alpha = e^4/(e^4 - 1)$.

For the second model, we take an oscillatory function $\gamma(t) = \frac{\cos(t)[-0.3\cos(t) - 2\sin(t)]}{e^{0.3t} - 2\cos(t)^2}$, which gives us

$$p_t = 1 - [e^{-0.3t}\cos(t)^2]. \tag{B7}$$

[1] Á. Rivas, S. F. Huelga, and M. B. Plenio, Quantum non-Markovianity: Characterization, quantification and detection, Rep. Prog. Phys. **77**, 094001 (2014).

[2] I. de Vega and D. Alonso, Dynamics of non-Markovian open quantum systems, Rev. Mod. Phys. **89**, 015001 (2017).

[3] J. Marshall, L. Campos Venuti, and P. Zanardi, Noise suppression via generalized-Markovian processes, Phys. Rev. A **96**, 052113 (2017).

[4] K. Siudzińska and D. Chruściński, Engineering fidelity of the generalized pauli channels via legitimate memory kernels, Phys. Rev. A **100**, 012303 (2019).

[5] C.-F. Li, G.-C. Guo, and J. Piilo, Non-Markovian quantum dynamics: What does it mean? Europhys. Lett. **127**, 50001 (2019).

[6] C.-F. Li, G.-C. Guo, and J. Piilo, Non-Markovian quantum dynamics: What is it good for? Europhys. Lett. **128**, 30001 (2020).

[7] M. Junge, R. Renner, D. Sutter, M. M. Wilde, and A. Winter, Universal recovery maps and approximate sufficiency of quantum relative entropy, Ann. Inst. Henri Poincaré **19**, 2955 (2018).

[8] M. M. Wilde, Recoverability in quantum information theory, Proc. R. Soc. A **471**, 20150338 (2015).

[9] D. Petz, Sufficient subalgebras and the relative entropy of states of a von Neumann algebra, Commun. Math. Phys. **105**, 123 (1986).

[10] D. Petz, Sufficiency of channels over von Neumann algebras, Quart. J. Math. Oxford Ser. (2) **39**, 97 (1988).

[11] A. Gilyén, S. Lloyd, I. Marvian, Y. Quek, and M. M. Wilde, Quantum algorithm for Petz recovery channels and pretty good measurements, arXiv:2006.16924.

[12] F. Buscemi, S. Das, and M. M. Wilde, Approximate reversibility in the context of entropy gain, information gain, and complete positivity, Phys. Rev. A **93**, 062314 (2016).

[13] S. Das, S. Khatri, G. Siopsis, and M. M. Wilde, Fundamental limits on quantum dynamics based on entropy change, J. Math. Phys. **59**, 012205 (2018).

[14] D. Sutter, M. Tomamichel, and A. W. Harrow, Strengthened monotonicity of relative entropy via pinched Petz recovery map, IEEE Trans. Inf. Theory **62**, 2907 (2016).

[15] H. Barnum and E. Knill, Reversing quantum dynamics with near-optimal quantum and classical fidelity, J. Math. Phys. **43**, 2097 (2002).

[16] S. Beigi, N. Datta, and F. Leditzky, Decoding quantum information via the Petz recovery map, J. Math. Phys. **57**, 082203 (2016).

[17] H. Kwon, R. Mukherjee, and M. S. Kim, Reversing Open Quantum Dynamics via Continuous Petz Recovery Map, Phys. Rev. Lett. **128**, 020403 (2022).

[18] A. M. Alhambra and M. P. Woods, Dynamical maps, quantum detailed balance, and the Petz recovery map, Phys. Rev. A **96**, 022118 (2017).

[19] H. K. Ng and P. Mandayam, Simple approach to approximate quantum error correction based on the transpose channel, Phys. Rev. A **81**, 062342 (2010).

[20] D. Chruściński, A. Rivas, and E. Stormer, Divisibility and Information Flow Notions of Quantum Markovianity for Non-invertible Dynamical Maps, Phys. Rev. Lett. **121**, 080407 (2018).

[21] J. Jeknic-Dugic, M. Arsenijevic, and M. Dugic, Invertibility as a witness of Markovianity of the quantum dynamical maps, arXiv:2012.08360.

[22] K. Siudzińska, Markovian semigroup from mixing noninvertible dynamical maps, Phys. Rev. A **103**, 022605 (2021).

[23] H. Breuer, P. Breuer, F. Petruccione, and S. Petruccione, *The Theory of Open Quantum Systems* (Oxford University, New York, 2002).

[24] J. Preskill, *Lecture Notes for Physics 229:Quantum Information and Computation* (CreateSpace Independent Publishing Platform, 2015).

[25] Á. Rivas and S. Huelga, *Open Quantum Systems: An Introduction*, Springer Briefs in Physics (Springer-Verlag, Berlin, 2011).

[26] H.-P. Breuer, E.-M. Laine, and J. Piilo, Measure for the Degree of Non-Markovian Behavior of Quantum Processes in Open Systems, Phys. Rev. Lett. **103**, 210401 (2009).

[27] D. Chruściński and F. A. Wudarski, Non-Markovian random unitary qubit dynamics, Phys. Lett. A **377**, 1425 (2013).

[28] M.-D. Choi, Completely positive linear maps on complex matrices, Linear Algebra and its Applications **10**, 285 (1975).

[29] I. Bengtsson and K. Zyczkowski, *Geometry of Quantum States: An Introduction to Quantum Entanglement* (Cambridge University, Cambridge, England, 2008), p. 860.

[30] C. Pineda, T. Gorin, D. Davalos, D. A. Wisniacki, and I. García-Mata, Measuring and using non-Markovianity, Phys. Rev. A **93**, 022117 (2016).